

Non-equilibrium GaNAs alloys with band gap ranging from 0.8–3.4 eV

K. M. Yu^{*1}, S. V. Novikov², R. Broesler^{1,3}, C. R. Staddon², M. Hawkrige¹, Z. Liliental-Weber¹, I. Demchenko^{4,5,6}, J. D. Denlinger⁴, V. M. Kao¹, F. Luckert⁷, R. W. Martin⁷, W. Walukiewicz¹, and C. T. Foxon²

¹ Materials Sciences Division, Lawrence Berkeley National Laboratory, 1 Cyclotron Road, Berkeley, CA 94720-8197, USA

² School of Physics and Astronomy, University of Nottingham, Nottingham NG7 2RD, UK

³ Department of Materials Science and Engineering, University of California, Berkeley, CA 94720, USA

⁴ Advanced Light Source, Lawrence Berkeley National Laboratory, 1 Cyclotron Road, Berkeley, CA 94720-8197, USA

⁵ Department of Chemistry, University of Nevada Las Vegas, 4505 Maryland Pkwy-Box 454003, Las Vegas, NV 89154-4003, USA

⁶ Institute of Physics, PAS, al. Lotnikow 32/46, 02-668 Warsaw, Poland

⁷ Department of Physics, SUPA, Strathclyde University, Glasgow G4 0NG, UK

Received 28 September 2009, revised 13 December 2009, accepted 13 December 2009

Published online 18 May 2010

Keywords GaNAs, MBE, structure, morphology, optical properties, band structure

* Corresponding author: e-mail kmyu@lbl.gov

A new alloy system, the GaN_{1-x}As_x alloys in the whole composition range was successfully synthesized using the non-equilibrium low temperature molecular beam epitaxy method. The alloys are amorphous in the composition range of 0.17 < x < 0.75 and crystalline outside this region. The amorphous films have smooth morphology, homogeneous composition and sharp, well defined opti-

cal absorption edges. The bandgap energy varies in a broad energy range from ~3.4 eV in GaN to ~0.8 eV at x ~ 0.85. The reduction of the band gap can be attributed primarily to the downward movement of the conduction band for alloys with x > 0.2, and to the upward movement of the valence band for alloys with x < 0.2.

© 2010 WILEY-VCH Verlag GmbH & Co. KGaA, Weinheim

1 Highly mismatched III-V alloys Semiconductor alloys formed through substitution of atoms with very different electronegativity and/or size have been known as highly mismatched alloys (HMAs) [1]. Because of large miscibility gaps, typically HMAs consist of a semiconductor matrix (elemental or compound) with the substitution of only a small amount (up to several percents) of distinctly different isovalent atoms. The HMAs show large band gap reduction and their electronic structures are drastically different from their host materials. A most notable example of HMAs is the As-rich GaN_xAs_{1-x} in which strong band gap reduction by as much as 180 meV per mole percent of N has been observed [2,3].

The unusually strong dependence of the fundamental gap on the N content in the group III-N-V alloys has been well described by the anticrossing interaction between localized N states and the extended conduction band states of the III-V matrix – the band anticrossing model (BAC) [1,3,4]. More recently, the BAC model has also been extended to HMAs where a small fraction of metallic isovalent atoms substitute more electronegative host atoms as occurs in the dilute N-rich GaN_{1-x}As_x alloys. In this case

due to the substantial difference in the ionization energies of the As and N anions, the As derived localized states interact strongly with the extended valence band states of the host. The interaction splits the valence band into a series of sub-bands with dispersion relations that are dependent on the As concentration [4,5].

2 Synthesis of GaNAs alloys Due to the large miscibility gap for the Ga-N-As system, GaNAs alloys with large compositions have not been achieved. It is known that in molecular beam epitaxy the As solubility limit in GaN_{1-x}As_x alloys is increasing with decreasing growth temperature [6]. In this study low temperature MBE (LT-MBE) has been employed to overcome the miscibility gap in the GaN_{1-x}As_x, allowing the synthesis of GaN_{1-x}As_x thin films over the whole composition range.

All GaNAs samples were grown on 2 inch sapphire (0001) substrates by plasma-assisted MBE at 100–600 °C. The same active N flux with the total N beam equivalent pressure (BEP) ~1.5 10⁻⁵ Torr and the same deposition time (2hr) were used for the majority of the films [7].

Report Documentation Page

Form Approved
OMB No. 0704-0188

Public reporting burden for the collection of information is estimated to average 1 hour per response, including the time for reviewing instructions, searching existing data sources, gathering and maintaining the data needed, and completing and reviewing the collection of information. Send comments regarding this burden estimate or any other aspect of this collection of information, including suggestions for reducing this burden, to Washington Headquarters Services, Directorate for Information Operations and Reports, 1215 Jefferson Davis Highway, Suite 1204, Arlington VA 22202-4302. Respondents should be aware that notwithstanding any other provision of law, no person shall be subject to a penalty for failing to comply with a collection of information if it does not display a currently valid OMB control number.

1. REPORT DATE OCT 2009		2. REPORT TYPE		3. DATES COVERED 00-00-2009 to 00-00-2009	
4. TITLE AND SUBTITLE Non-equilibrium GaNAs alloys with band gap ranging from 0.8-3.4 eV				5a. CONTRACT NUMBER	
				5b. GRANT NUMBER	
				5c. PROGRAM ELEMENT NUMBER	
6. AUTHOR(S)				5d. PROJECT NUMBER	
				5e. TASK NUMBER	
				5f. WORK UNIT NUMBER	
7. PERFORMING ORGANIZATION NAME(S) AND ADDRESS(ES) Lawrence Berkeley National Laboratory, Materials Sciences Division, 1 Cyclotron Road, Berkeley, CA, 94720-8197				8. PERFORMING ORGANIZATION REPORT NUMBER	
9. SPONSORING/MONITORING AGENCY NAME(S) AND ADDRESS(ES)				10. SPONSOR/MONITOR'S ACRONYM(S)	
				11. SPONSOR/MONITOR'S REPORT NUMBER(S)	
12. DISTRIBUTION/AVAILABILITY STATEMENT Approved for public release; distribution unlimited					
13. SUPPLEMENTARY NOTES See also ADM002356. Presented at the International Conference on Nitride Semiconductors (8th) (ICNS8) Held in Jeju, Korea on October 18-23, 2009. Sponsored by AOARD.					
14. ABSTRACT					
15. SUBJECT TERMS					
16. SECURITY CLASSIFICATION OF:			17. LIMITATION OF ABSTRACT Same as Report (SAR)	18. NUMBER OF PAGES 3	19a. NAME OF RESPONSIBLE PERSON
a. REPORT unclassified	b. ABSTRACT unclassified	c. THIS PAGE unclassified			

The composition of the films was measured by Rutherford backscattering spectrometry (RBS) and particle induced x-ray emission (PIXE). Composition mapping by wavelength-dispersive x-ray spectroscopy with $\sim 1 \mu\text{m}$ resolution further confirms the composition and found no discernable compositional variation over a $256 \times 256 \mu\text{m}$ region in the films. Figure 1 shows the As composition in $\text{GaN}_{1-x}\text{As}_x$ films as a function of growth temperature. The Ga and As_2 flux in these growths were kept constant with BEP $\sim 1.5 \times 10^{-7}$ and $\sim 7.5 \times 10^{-6}$ Torr, respectively. A monotonic increase in the As incorporation in the film is observed as the growth temperature is reduced. We note that as the growth temperature decreases, along with the increase in As content in the film, the film loses its crystallinity and becomes amorphous (close circle symbols in Fig. 1).

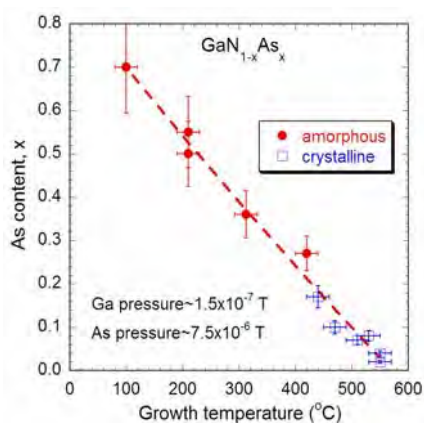


Figure 1 The Arsenic composition in $\text{GaN}_{1-x}\text{As}_x$ films grown by LT-MBE measured by RBS/PIXE as a function of growth temperature.

3 Structural and optical properties X-ray diffraction measurements show that as the growth temperature is reduced from ~ 600 to $100 \text{ }^\circ\text{C}$, along with the increase in the As incorporation from $x \sim 0.02$ to 0.7 , the structure of the $\text{GaN}_{1-x}\text{As}_x$ film transforms from crystalline (wurtzite) to amorphous ($< 410 \text{ }^\circ\text{C}$). This is further confirmed by selective area electron diffraction (SAD) studies shown in Fig. 2. The SAD results unambiguously illustrate that the $\text{GaN}_{1-x}\text{As}_x$ alloys go from single crystalline spot pattern ($T_g = 550 \text{ }^\circ\text{C}$) to polycrystalline ring pattern ($400 \text{ }^\circ\text{C} < T_g < 500 \text{ }^\circ\text{C}$) to amorphous diffuse ring pattern ($T_g < 400 \text{ }^\circ\text{C}$; $x > 0.2$). The diffuse ring patterns for $\text{GaN}_{1-x}\text{As}_x$ alloys with x in the range of ~ 0.2 to 0.75 confirm the amorphous structure of these alloys. The As content in the amorphous film can also be increased by increasing the As flux during growth. This is shown in Fig. 2 with the SAD patterns from two amorphous samples grown at $210 \text{ }^\circ\text{C}$: the sample with 45% As was grown with $\sim 6\times$ higher As flux as the sample with 27% As. High resolution transmission electron microscopy on the high As content $\text{GaN}_{1-x}\text{As}_x$ layer

(45% As) clearly shows a homogeneous, amorphous film with no observable composition segregation.

As the alloy composition is pushed to the As-rich side ($x > 0.75$) the films becomes crystalline again with a cubic structure. The SAD pattern for the As-rich $\text{GaN}_{1-x}\text{As}_x$ film with $x = 0.86$ grown at $\sim 200 \text{ }^\circ\text{C}$ is shown in Fig. 2. The ring pattern of this sample is consistent with the XRD result that shows a cubic polycrystalline phase of $\text{GaN}_{1-x}\text{As}_x$ for As-rich alloys $\sim 14\%$ N substituting the As sublattice.

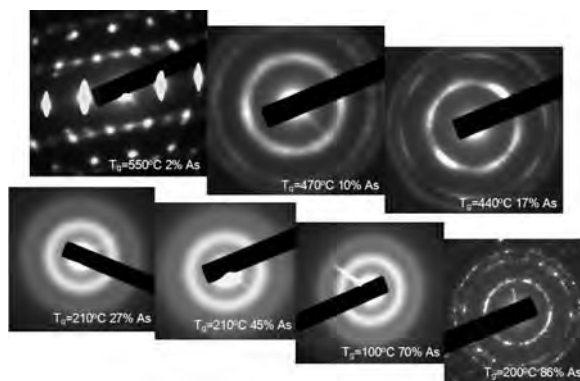


Figure 2 A series of selective area electron diffraction pattern (SAD) from $\text{GaN}_{1-x}\text{As}_x$ alloys with increasing As content as a result of decreasing growth temperature from 550 to $100 \text{ }^\circ\text{C}$.

Optical absorption measurements show a strikingly sharp band gap absorption in all films. Despite the crystalline and amorphous transition a continuously monotonic decrease in the band gap is observed as the As content increases. This also supports the claim that the films are single phase with no phase separation in the crystalline state, and no composition non-uniformity in the amorphous state.

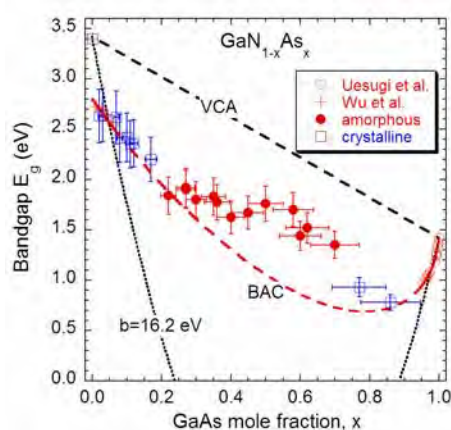


Figure 3 Dependence of the optical band gap energy obtained by absorption measurements on the value of x for crystalline and amorphous $\text{GaN}_{1-x}\text{As}_x$ alloys.

Figure 3 summarizes the composition dependence of the optical band gap energy for both crystalline (open

symbols) and amorphous (solid symbols) $\text{GaN}_{1-x}\text{As}_x$ alloys. These experimental data are compared directly with calculated composition dependence of the band gap. It is obvious that these data cannot be explained by a virtual crystal approximation (VCA) represented by the dashed line. The dotted line in Fig. 3 shows a forced quadratic fitting to the experimental gap energies on dilute alloys with a single bowing parameter of $b=16.2$ eV. Excellent agreement can be observed between the band gap values for the crystalline alloys and the BAC model. The deviation of the experimental results from the BAC calculations found for the amorphous alloys is not unexpected as the model has been developed for crystalline materials.

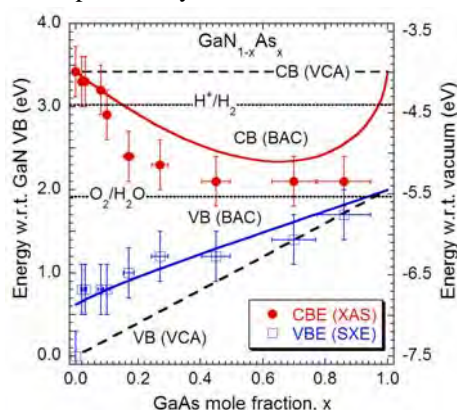


Figure 4 Composition dependence of the conduction band minimum (CBM) and the valence band maximum (VBM) energies for $\text{GaN}_{1-x}\text{As}_x$ alloys as measured by XAS and SXE, respectively.

To directly measure the band positions we used the combination of soft x-ray emission (SXE) and absorption (XAS) spectroscopies. XAS and SXE directly probe the partial density of states (DOS) of the conduction band and valence band, respectively [8]. The composition dependence of the CBE and the VBE energies for $\text{GaN}_{1-x}\text{As}_x$ alloys as measured by XAS and SXE, respectively, is shown in Fig. 4 together with the BAC predicted values. The linear interpolations of CBE and VBE (VCA) between end point binary compounds (GaN and GaAs) are also shown. Figure 4 shows that both CBE and VBE are shifted as x increases. In general, the experimental CBE and VBE values significantly but follow the trend of the BAC prediction, although the alloys with composition in the range of $x \sim 0.2$ – 0.75 are amorphous.

4 Conclusion We have successfully synthesized $\text{GaN}_{1-x}\text{As}_x$ alloys in the whole composition range using low temperature molecular beam epitaxy. Alloys in the composition range of $0.17 < x < 0.75$ are amorphous with no indication of composition non-uniformity. Optical absorption measurements show sharp absorption edges with a gradual decrease of the bandgap from ~ 3.4 eV to < 1 eV with increasing As content. The energy gap reaches its minimum of ~ 0.8 eV at $x \sim 0.8$. The composition depend-

ence of the band gap of the crystalline $\text{GaN}_{1-x}\text{As}_x$ alloys ($x < 0.2$ and $x > 0.8$) follows the prediction of the band anticrossing model well while the amorphous alloys show higher band gaps than predicted (by as much as ~ 0.6 eV). The reduction of the band gap can be attributed primarily to the downward movement of the conduction band minimum for alloys with $x > 0.2$, and to the upward movement of the valence band maximum for alloys with $x < 0.2$.

The unusual electronic structure and capability for controlling the locations of the conduction and valence band edges offer unprecedented opportunity for using these alloys for novel solar power conversion devices. For example, we propose that the N-rich $\text{GaN}_{1-x}\text{As}_x$ alloys can be promising materials for the photoanodes for the direct conversion of sunlight into hydrogen by photoelectrochemical (PEC) water-splitting. Moreover, the wide band gap tuneability of this alloy system covering a spectral range of ~ 0.8 to 3.4 eV provides an almost perfect match to the solar spectrum. This offers the opportunity to design high efficiency multijunction solar cells using a single ternary alloy system.

Acknowledgements This work was supported by the Director, Office of Science, Office of Basic Energy Sciences, Materials Sciences and Engineering Division, of the U.S. Department of Energy under Contract No. DE-AC02-05CH11231. The work at the University of Nottingham was undertaken with support from the EPSRC (EP/G007160/1 and EP/D051487/1).

References

- [1] W. Walukiewicz, W. Shan, K. M. Yu, J. W. Ager III, E. E. Haller, I. Miotkowski, M. J. Seong, H. Alawadhi, and A. K. Ramdas, *Phys. Rev. Lett.* **85**, 1552 (2000).
- [2] K. Uesugi, N. Marooka, and I. Suemune, *Appl. Phys. Lett.* **74**, 1254 (1999).
- [3] W. Shan, W. Walukiewicz, J. W. Ager III, E. E. Haller, J. F. Geisz, D. J. Friedman, J. M. Olson, and S. R. Kurtz, *Phys. Rev. Lett.* **82**, 1221 (1999).
- [4] W. Walukiewicz, K. Alberi, J. Wu, W. Shan, K.M. Yu, and J. W. Ager III, in *Physics of Dilute III-V Nitride Semiconductors and Material Systems: Physics and Technology*, edited by Ayse Erol (Springer-Verlag, Berlin-Heidelberg, 2008), Chap. 3.
- [5] J. Wu, W. Walukiewicz, K. M. Yu, J. D. Denlinger, W. Shan, J. W. Ager, A. Kimura, H. F. Tang, and T. F. Kuech, *Phys. Rev. B* **70**, 115214, (2004).
- [6] S. V. Novikov, T. Li, A. J. Winsor, R. P. Campion, C. R. Staddon, C. S. Davis, I. Harrison, and C. T. Foxon, *Phys. Status Solidi B* **228**, 223 (2001).
- [7] S. V. Novikov, C. R. Staddon, A. V. Akimov, R. P. Campion, N. Zainal, A. J. Kent, C. T. Foxon, C.-H. Chen, K. M. Yu, and W. Walukiewicz, *J. Cryst. Growth* **311**, 3417 (2009).
- [8] L. C. Duda, C. B. Stagarescu, J. Downes, K. E. Smith, D. Korakakis, T. D. Moustakas, J. H. Guo, and J. Nordgren, *Phys. Rev. B* **58**, 1928 (1998).